

Multiphoton intrapulse interference. IV. Ultrashort laser pulse spectral phase characterization and compensation

Vadim V. Lozovoy, Igor Pastirk, and Marcos Dantus

Department of Chemistry and Physics, Michigan State University, East Lansing, Michigan 48824-1322

Received August 4, 2003

We introduce a noninterferometric single beam method to characterize and compensate the spectral phase of ultrashort femtosecond pulses accurately. The method uses a pulse shaper that scans calibrated phase functions to determine the unknown spectral phase of a pulse. The pulse shaper can then be used to synthesize arbitrary phase femtosecond pulses or it can introduce a compensating spectral phase to obtain transform-limited pulses. This method is ideally suited for the generation of tailored spectral phase functions required for coherent control experiments. © 2004 Optical Society of America

OCIS codes: 320.5540, 320.7100, 320.7110.

Accurate measurement of the spectral phase in femtosecond laser pulses is the key for pulse compression or generation of phase-modulated pulses as required for femtochemistry,¹ coherent control of chemical reactions^{2,3} and optical communications.⁴ There are currently a number of methods to measure the spectral phase of ultrashort pulses, among the most salient are frequency resolved optical gating⁵ (FROG) and spectral phase interferometry for direct electric-field reconstruction.⁶ Similarly, there are a number of methods for shaping the phase of a femtosecond pulse.⁷ Ideally, characterization and pulse-shaping instruments can work together to produce transform-limited (TL) or precisely phase-shaped pulses. Attempts to merge pulse shaping and characterization have used either a genetic algorithm controlled shaper to optimize a nonlinear optical signal^{8,9} or implemented time-domain interferometry with an acousto-optic programmable filter.¹⁰ Here we present an accurate method that combines spectral phase characterization with pulse shaping in one simple setup. The method, multiphoton intrapulse interference phase scan (MIIPS), takes advantage of the influence that phase modulation has on the probability of nonlinear optical processes at specific frequencies.¹¹⁻¹⁴ This method has already proved extremely powerful for the demonstration of selective multiphoton microscopy by use of ultrashort shaped pulses.¹⁵

The second-harmonic generation (SHG) spectrum $S^{(2)}(\Delta)$ at a frequency $2(\omega_0 + \Delta)$ is written as an integral over the frequency-dependent amplitude $|E(\Delta)|$ and phase $\varphi(\Delta)$, according to

$$S^{(2)}(\Delta) \propto \left| \int |E(\Delta + \Omega)| |E(\Delta - \Omega)| \times \exp\{i[\varphi(\Delta + \Omega) + \varphi(\Delta - \Omega)]\} d\Omega \right|^2. \quad (1)$$

Expression (1) connects the spectral phase of the pulse to its second-harmonic spectrum. If we consider a Taylor expansion of the spectral phase near Δ , only nonzero even terms of the expansion

can decrease $S^{(2)}$ at Δ . Because of cancellation of the interference term $\varphi(\Delta + \Omega) + \varphi(\Delta - \Omega)$ in Eq. (1) for second-order processes, $S^{(2)}(\Delta)$ is not affected by the common phase $\varphi^{(0)}$ or by the odd terms $\varphi'\Omega, \varphi'''\Omega^3, \dots$

Phase retrieval by use of a MIIPS involves the introduction of reference phases given by $f(\Delta)$ that reduce or cancel phase distortions in one or more regions of the spectrum to determine the unknown phase $\phi(\Delta)$. Maximum SHG signals are observed when phase distortions in the output phase $\varphi(\Delta) = \phi(\Delta) + f(\Delta)$ are minimized. This condition is found when all even terms in the Taylor expansion for ϕ and f cancel each other. The leading terms define the condition when the second derivative of the phase equals zero:

$$\varphi''(\Delta) = \phi''(\Delta) + f''(\Delta) = 0. \quad (2)$$

Given that the second derivative of the reference function $f(\Delta)'' \equiv d^2f(\Omega)/d\Omega^2|_{\Delta}$ is known, we can determine $\phi(\Delta)'' \equiv d^2\phi(\Omega)/d\Omega^2|_{\Delta}$.

Equation (2) gives the condition when the nonlinear signal generated at frequency Δ has a maximum. We use the function $f(\Delta) = \alpha \cos(\gamma\Delta - \delta)$ to generate the reference functions. Scanning the parameter δ and collecting the SHG spectrum for each value generates the two-dimensional MIIPS trace from which one can find the condition $\delta_{\max}(\Delta)$ when the maximum SHG signal is obtained. The second derivative of the reference function where the maximum signal is observed is given by $f''(\Delta) = -\alpha\gamma^2 \cos[\gamma\Delta - \delta_{\max}(\Delta)]$. We introduce this expression into Eq. (2) to obtain

$$\phi''(\Delta) = -f''(\Delta) = \alpha\gamma^2 \cos[\gamma\Delta - \delta_{\max}(\Delta)], \quad (3)$$

a formula used to retrieve the second derivative of the unknown spectral phase $\phi(\Delta)$ directly by integration of $\phi''(\Delta)$ over frequency Δ . The unknown constants of integration, $\phi^0(\Delta)$ and $\phi'(\Delta)$, are set to zero.

Once $\phi(\Delta)$ is determined, a compensation phase function equal to $-\phi(\Delta)$ is introduced to cancel the original phase modulation and to obtain TL pulses. For TL pulses $\phi''(\Delta) = 0$, and the solution of Eq. (3)

for δ_{TLmax} is given by $\delta_{\text{TLmax}}(\Delta) = \gamma\Delta \pm \pi/2$, which rigorously establishes that TL pulses are characterized by parallel lines separated by π , described by $\delta_{\text{max}}(\lambda)$ in the δ, λ plane [$\lambda = \pi c/(\omega_0 + \Delta)$]. When the only phase distortion is linear chirp, the parallel lines $\delta_{\text{max}}(\lambda)$ are no longer spaced by π . Cubic phase modulation (quadratic chirp) causes a change in the slope of $\delta_{\text{max}}(\lambda)$. Therefore, one can quickly and intuitively determine the sign and approximate amplitude of phase distortions in a laser pulse by inspection of a MIIPS trace.

The analysis presented above did not take into account higher-order phase modulation terms. The higher-order terms in the Taylor expansion of functions f and ϕ lead to cumulative systematic errors in the measurement of ϕ_{meas}'' that is defined by $\phi_{\text{meas}}'' = (1 + \epsilon_f + \epsilon_\phi)\phi''$ and are given by $\epsilon_f \approx \sum_n 2(\gamma\sigma)^{n-2}/n!$ and $\epsilon_\phi \approx \sum_n 2(\phi^{(n)}\sigma^{n-2})/n!$ for even $n > 2$. Errors from high-order phase terms ϵ_ϕ scale with spectral width σ . Errors that are due to high-order distortions in ϵ_f become exponentially small for $\gamma\sigma < 1$. As long as $\gamma\sigma \approx 1$, the first term in ϵ_f is the largest source of error and is approximately 10%. A simple iterative measurement and compensation process is used to eliminate these errors. The goal is to introduce increasingly fine compensation functions $\phi^n(\Delta)$ until TL pulses are obtained according to

$$\phi(\Delta) - [\phi^I(\Delta) + \phi^{II}(\Delta) + \phi^{III}(\Delta) + \dots] \approx 0. \quad (4)$$

The N th correction term is obtained by measurement of a MIIPS trace, determination of $\delta_{\text{max}}(\Delta)$, and retrieval of $\phi^N(\Delta)$, a function that is added in the spatial light modulator (SLM) for phase compensation. After two or three iterations, the cumulated phase according to approximation (4) corresponds to the accurate phase $\phi(\Delta)$ across the spectrum.

The experimental setup for the MIIPS is straightforward, requiring only a thin SHG crystal and a spectrometer (see Fig. 1), provided that a pulse shaper is already available. The method is not based on autocorrelation, therefore, no overlap of beams in time or space is required, nor are symmetric scans dependent on the spatial mode or tweaking of the beam's intensity and pointing. The MIIPS method can be easily carried out at the location of the sample. The measurements presented here were carried out by use of sub-20-fs pulses from a Ti:sapphire oscillator (K&M Laboratories). The pulse energy was attenuated down to ~ 3 nJ. A $15\text{-}\mu\text{m}$ β -barium borate type I crystal was used for SHG, and the output was attenuated and directed to a spectrometer. The pulse shaper is based on the general design of Weiner *et al.*¹⁶ having two prisms, two cylindrical mirrors (200-mm focal length), and a SLM consisting of two 128 LCD elements (CRL, Inc., SLM-256). We carefully calibrated the shaper by measuring the polarization-dependent transmission to provide accurate phase delays (better than 1 deg). The calibration was carried out for each pixel of the double-mask pulse shaper because, for short enough pulses (< 30 fs), frequency-dependent changes in the index of refraction must be taken

into account. We used the method with amplified (1-mJ, ~ 50 -fs) pulses (not shown here) with minor alterations. SHG FROG measurements were also obtained to corroborate our results by use of the same thin SHG crystal.

The experimental results in Fig. 2 correspond to pulses with significant spectral phase distortion. The two-dimensional contour plot (Fig. 2a) is the MIIPS trace corresponding to the SHG spectrum as a function of δ . The diagonal lines were obtained from a simple algorithm that determines the local maximum of the signal for each δ . From the curvature and slope of these lines, which describe δ_{max} versus λ , one obtains the second derivative of phase distortion $\phi''(\Delta)$ according to Eq. (3) and the first approximation for phase $\phi(\Delta)$ after double integration. This first retrieved phase $\phi^I(\Delta)$ is shown in Fig. 2b as a thin solid curve. We programmed the SLM to compensate this phase and obtained a new MIIPS trace to obtain the next correction $\phi^{II}(\Delta)$. The cumulative phases from four such iterations are presented in Fig. 2. The final phase, $\phi(\Delta) = \phi^I(\Delta) + \phi^{II}(\Delta) + \phi^{III}(\Delta) + \phi^{IV}(\Delta)$, is shown in Fig. 2b as a thick solid curve. A SHG FROG trace of the same pulses is shown in Fig. 2c. The retrieved phase (dashed curve) and spectrum (thin curve) are shown in Fig. 2d.

Having retrieved $\phi(\Delta)$, we introduced a compensation phase equal to $-\phi(\Delta)$ to obtain 19-fs TL pulses as shown in Fig. 3. The measured MIIPS is shown in Fig. 3a, where one can see the equidistant straight parallel lines that characterize TL pulses. The spectrum of the pulse and residual phase across the spectrum is shown in Fig. 3b. The phase axis has been scaled by 1/100 to reveal the measured residual phase distortion of $\sim \pm 0.01$ rad. A SHG FROG trace of the compensated pulses is shown in Fig. 3c, and the retrieved

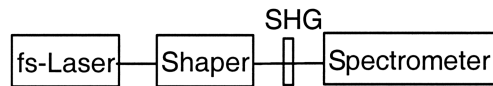


Fig. 1. Experimental setup of the MIIPS.

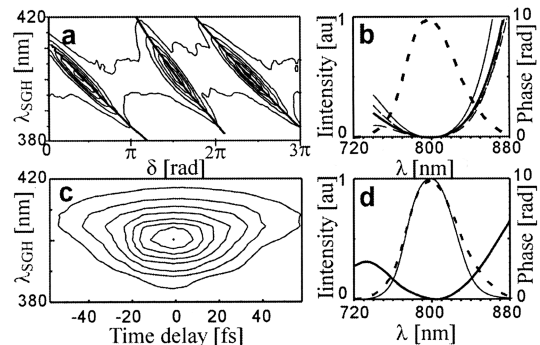


Fig. 2. a, Experimental MIIPS data obtained for phase-distorted pulses. The SHG intensity as a function of wavelength λ and reference phase position δ is given by the contours. The lines are the local maxima in the MIIPS trace. b, Measured spectral intensity (dashed) and phases retrieved after the first (thin) to final fourth iteration (thick). c, SHG FROG for the same pulses. d, Measured (dashed) and retrieved spectrum (thin) and phase (thick) from SHG FROG measurements.

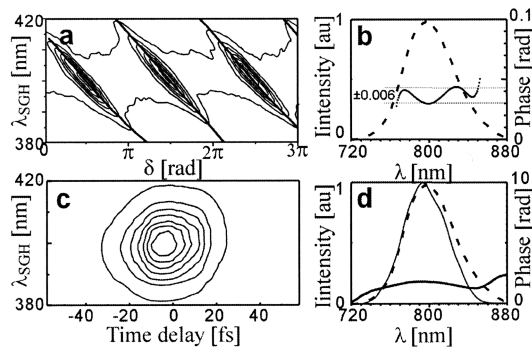


Fig. 3. a, Experimental MIIPS data obtained for phase-compensated TL pulses. b, Measured spectral intensity (dashed) and phase retrieved (thick). c, SHG FROG for the same pulses. d, Measured (dashed) and retrieved spectrum (thin) and phase (thick) from SHG FROG measurements. Note the change in scales for the phase measurements.

phase and spectrum in Fig. 3d. Analysis of the SHG FROG was carried out with the commercial software package Femtosoftware, with an overall lower precision and accuracy than that obtained with the MIIPS.

The resolution and range of the MIIPS method are directly proportional to the reference function parameters; therefore, they are adjusted for different experiments as needed. The operable range is given by $|\phi''| > \alpha\gamma^2$. Experimentally we have found the precision of MIIPS measurements to be within 0.01 rad across the spectrum of the pulse, and the overall accuracy within 0.1 rad across the spectrum. We have not obtained that level of precision from FROG with which the fitting choices and signal preprocessing can influence the final retrieved phase. The degree of complexity of the waveform that can be measured with the MIIPS depends on the second derivative of the phase because it describes the rate of change of the phase across the spectrum. If the second derivative satisfies $|\phi''(\Delta)| < \alpha\gamma^2$, the phase can be measured and compensated. The best results are found for $\gamma = \tau$, the pulse duration. For pulses used in these experiments $\gamma = 20$ fs and $\alpha = 5$, giving an upper limit to the local phase curvature $\phi'' \sim 2000$ fs². The MIIPS can be tailored to compensate very small (0.01 rad) or very large (10 rad, shaper limited) distortions. Characterization of arbitrarily complex pulses with discontinuities across the spectrum is extremely challenging. These types of pulse are typically generated by pulse shapers under the control of a genetic

algorithm.^{2,3} We use the MIIPS to obtain TL pulses and then let the genetic algorithm modify the phase to achieve a specific target. Because the starting phase is known and the shaper is calibrated, the final phase can be read directly from the pulse shaper.

We have introduced and demonstrated a method to characterize the spectral phase of femtosecond pulses. This single beam method is capable of retrieving arbitrary spectral phases with high resolution. Pulse retrieval is based on analytical expressions that yield the spectral phase directly from the experimental data.

This research was funded by the Chemical Sciences, Geosciences, and Biosciences Division, Office of Basic Energy Sciences, Office of Science, U.S. Department of Energy. National Science Foundation grant CHE-0135581 has supported I. Pastirk. M. Dantus's e-mail address is dantus@msu.edu.

References

1. A. H. Zewail, *Angew. Chem. Int. Ed. Engl.* **39**, 2587 (2000).
2. A. Assion, T. Baumert, M. Bergt, T. Brixner, B. Kiefer, V. Seyfried, M. Strehle, and G. Gerber, *Science* **282**, 919 (1998).
3. R. J. Levis, G. M. Menkir, and H. Rabitz, *Science* **292**, 709 (2001).
4. Z. Zheng and A. M. Weiner, *Chem. Phys.* **267**, 161 (2001).
5. R. Trebino, K. W. DeLong, D. N. Fittinghoff, J. N. Sweetser, M. A. Krumbügel, B. A. Richman, and D. J. Kane, *Rev. Sci. Instrum.* **68**, 3277 (1997).
6. C. Iaconis and I. A. Walmsley, *Opt. Lett.* **23**, 792 (1998).
7. A. M. Weiner, D. E. Leaird, J. S. Patel, and J. R. Wullert II, *IEEE J. Quantum Electron.* **28**, 908 (1992).
8. A. Efimov and D. H. Reitze, *Opt. Lett.* **23**, 1612 (1998).
9. E. Zeek, K. Maginnis, S. Backus, U. Russek, M. Murnane, G. Mourou, H. Kapteyn, and G. Vdovin, *Opt. Lett.* **24**, 493 (1999).
10. A. Monmayrant, M. Joffre, T. Oksenhendler, R. Herzog, D. Kaplan, and P. Tournois, *Opt. Lett.* **28**, 278 (2003).
11. B. Broers, H. B. van Linden van den Heuvell, and L. D. Noordam, *Opt. Commun.* **91**, 57 (1992).
12. K. A. Walowicz, I. Pastirk, V. V. Lozovoy, and M. Dantus, *J. Phys. Chem. A* **106**, 9369 (2002).
13. V. V. Lozovoy, I. Pastirk, K. A. Walowicz, and M. Dantus, *J. Chem. Phys.* **118**, 3187 (2003).
14. M. Hacker, R. Netz, M. Roth, G. Stobrawa, T. Feurer, and R. Sauerbrey, *Appl. Phys. B* **73**, 273 (2001).
15. I. Pastirk, J. M. Dela Cruz, K. A. Walowicz, V. V. Lozovoy, and M. Dantus, *Opt. Express* **11**, 1695 (2003), <http://www.opticsexpress.org>.
16. A. M. Weiner, *Rev. Sci. Instrum.* **71**, 1929 (2000).